

# Eutectic Solidification in the System $\text{Al}_2\text{O}_3/\text{Y}_3\text{Al}_5\text{O}_{12}$

D. VIECHNICKI, F. SCHMID

*Army Materials and Mechanics Research Center, Watertown, Mass, USA*

*Received 12 August 1968*

The eutectic solidification in the system  $\text{Al}_2\text{O}_3/\text{Y}_3\text{Al}_5\text{O}_{12}$  has been investigated. A Bridgman-type crystal-growing furnace was used in this investigation. A temperature gradient of  $190^\circ\text{C}/\text{cm}$  and growth rates which were varied between 2 and 12 cm/h were employed in the directional solidification studies. Three types of microstructure were observed depending upon the composition and the growth rate. At a growth rate of 4 cm/h and at compositions removed from the eutectic composition, a mixture of primary phase and fine eutectic dispersion was found. At growth rates between 2 and 12 cm/h at the eutectic composition, a colony type microstructure was most commonly observed. At growth rates above 4 cm/h at the eutectic composition, regions in the solidified ingot were found to have a highly oriented eutectic microstructure consisting of both rods and platelets. These eutectic microstructures indicate that coupled growth can occur in this system. The method of Sunquist and Mondolfo [15] was used to determine whether  $\text{Y}_3\text{Al}_5\text{O}_{12}$  was the first phase to nucleate at the eutectic.

## 1. Introduction

Eutectic microstructures may be classified according to the growth characteristics of their component phases, i.e. non-faceted/non-faceted, non-faceted/faceted, and faceted/faceted [1]. Hunt and Jackson [2] have further suggested that eutectic microstructures may be classified according to the entropies of melting of the component phases. They found for several organic systems that those with an entropy of melting below  $2R$ , where  $R$  is the Universal Gas Constant, exhibited eutectic growth whereas those with an entropy of melting greater than  $2R$  exhibited microstructures consisting of fine dispersions of independent crystals. Chadwick [1] has given examples of several exceptions to this latter method of classification in metal systems. While much work has been done on solidification in metal systems which have a low entropy of melting, little work has been done on solidification in oxide systems, which generally exhibit a high entropy of melting and faceted growth from the melt. The object of this investi-

gation was to study the microstructures produced by solidification in the system  $\text{Al}_2\text{O}_3/\text{Y}_3\text{Al}_5\text{O}_{12}$  and to determine whether coupled eutectic growth is possible in this system. The system  $\text{Al}_2\text{O}_3/\text{Y}_3\text{Al}_5\text{O}_{12}$  was chosen because both  $\text{Al}_2\text{O}_3$  and  $\text{Y}_2\text{O}_3$  have low vapour pressures below  $2000^\circ\text{C}$  [3] and are not easily reduced to suboxides [4, 5].

The entropy of melting of  $\text{Al}_2\text{O}_3$  is  $6.2R$  [6] and that of  $\text{Y}_3\text{Al}_5\text{O}_{12}$  may be assumed to be greater than  $2R$  although no data is available in the literature. Both  $\text{Al}_2\text{O}_3$  and  $\text{Y}_3\text{Al}_5\text{O}_{12}$  usually yield faceted single crystals when pulled from the melt [7, 8]. The volume ratio of  $\text{Y}_3\text{Al}_5\text{O}_{12}$  to  $\text{Al}_2\text{O}_3$  at the eutectic composition is 0.44 [9].

## 2. Experimental

### 2.1. Materials

The starting materials used in this investigation were high-purity alumina\* and yttria†. The alumina powder contained greater than 99.99%  $\text{Al}_2\text{O}_3$ . Typical impurities listed by the producer were less than 0.003%  $\text{Na}_2\text{O}$ , less than 0.0015%

\*Gem-242 Ultra High Purity Alumina, Engineering Materials, PO Box 363, New York 8, New York, USA

†Trona 1116 Yttria, American Potash and Chemical Corp, Rare-Earth Division, 258 Ann St, West Chicago, Ill, USA

$\text{SiO}_2$ , less than 0.001%  $\text{TiO}_2$ , less than 0.001%  $\text{Fe}_2\text{O}_3$ , less than 0.001%  $\text{P}_2\text{O}_5$ , and less than 0.001% Cl. The yttria powder contained greater than 99.99%  $\text{Y}_2\text{O}_3$ . Typical impurities listed by the producer included traces of all the rare-earth oxides. Major non-rare-earth impurities were CaO, MgO, and  $\text{SiO}_2$  totalling not more than 0.002%. These powders were weighed in proper proportions, mixed in a blender for 1 h in acetone, dried, and calcined for more than 60 h at  $1000^\circ\text{C}$ . The calcined powders were then either put directly in a vacuum furnace for solidification studies or stored in an evacuated desiccator.

## 2.2. Directional Solidification

Cylindrical vapour deposited tungsten crucibles\* 1.90 cm in diameter by 15.25 cm in height were used throughout the investigation. Melting and solidification were accomplished under vacuums of less than  $1.5 \times 10^{-2}$  torr in a Bridgman type crystal-growing furnace shown schematically in fig. 1. Power was supplied by a 450 kHz 20 kW rf generator, and heating was accomplished by coupling directly to the crucible. Melts of the eutectic composition were heated to  $1830^\circ\text{C}$ ,  $30^\circ$  above their melting point [9], and melts of compositions other than the eutectic composition were heated to about  $50^\circ$  above what were estimated to be their melting points although no attempt was made to determine these melting points. Directional solidification was accomplished by passing the crucible down through the coils after the lower zirconia heat shield (fig. 1) was pulled down and out of the line of sight of the pyrometer. Cooling was accomplished by radiation from the bottom of the crucible. Temperatures were measured from the bottom of the crucible with an optical pyrometer which had been previously calibrated against a standard tungsten lamp. Corrections for losses of radiation because of the vitreous silica sight port window and the prism, emissivity of the tungsten, and temperature gradient through the base of the crucible were applied to the observed temperature to obtain the temperature of the material. This corrected temperature agreed well with the melting temperature of these materials found with another technique [9]. The temperature gradient in the liquid could only be obtained at the beginning of directional solidification. The initial temperature was taken from the crucible bottom just after the lower zirconia heat shield was pulled away. This temperature was

\*San Fernando Laboratories, 10258 Norris St, Pacoima, Cal, USA

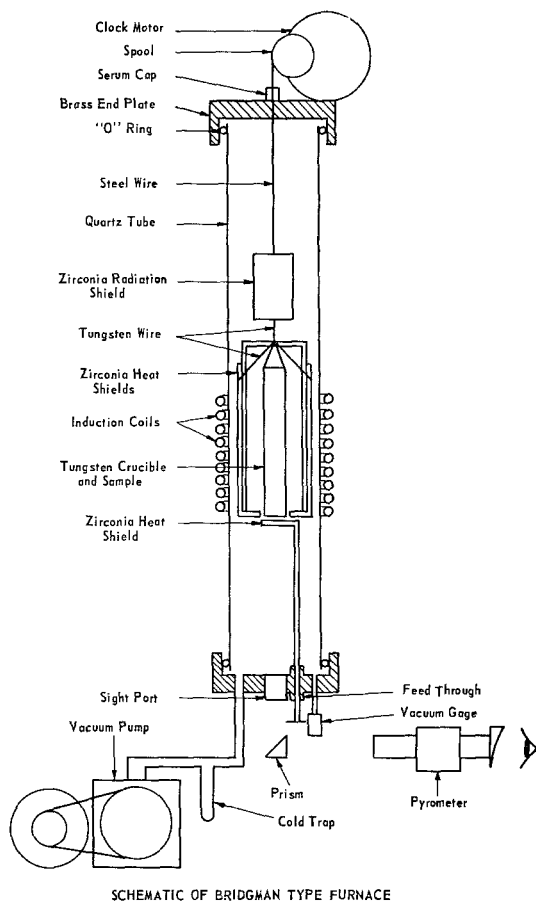


Figure 1 Schematic of Bridgman type furnace. Lower zirconia heat shield moves down and out of the line of sight of the pyrometer during solidification.

assumed to be the temperature of the melt throughout solidification. Subsequent temperatures were taken as the crucible dropped. These subsequent temperatures that were still above the melting point were subtracted from the initial temperature. This temperature change was then divided by the distance the crucible had dropped to give the temperature gradient in the liquid. The temperature gradient was found to be  $190^\circ\text{C}/\text{cm}$  for this particular furnace arrangement at the start of directional solidification. The temperature gradient probably decreased during solidification, but this could not be determined. Growth rate was varied between 2 and 12 cm/h by changing the diameter of the spool around which the wire was wrapped (fig. 1).

### 2.3. Optical Studies

Photomicrographs were obtained from a Bausch and Lomb metallograph with a carbon arc light source. Prints were made from glass plates. Graded silicon carbide papers, diamond paste, and final relief polish with chromic oxide were used to prepare the polished sections.

### 3. Results and Discussion

When a microstructure free of primary  $Y_3Al_5O_{12}$  could not be obtained from the eutectic compositions reported in the literature [10-13], the position of the eutectic point was re-investigated and found to lie at 80.1 mol %  $Al_2O_3$ /19.9 mol %  $Y_3Al_5O_{12}$  (81.3 mol %  $Al_2O_3$ /18.7 mol %  $Y_2O_3$ ) at 1800° C [9].

Several compositions in the system  $Al_2O_3/Y_3Al_5O_{12}$  were directionally solidified with a temperature gradient of 190° C/cm in the liquid and at growth rates varying from 2 to 12 cm/h. Ingots consisted of large columnar grains, about 0.3 by 3 cm, nucleated at the bottom of the ingot. Ingots were free of porosity arising from entrapped gases and dispersed porosity arising from the difference in volume between liquid and solid. The difference in volume between liquid  $Al_2O_3$  and solid  $Al_2O_3$  at the melting point has been reported to be 22% [14]. Three different types of microstructures were observed within the columnar grains depending upon the composition of the ingot and the growth rate. At a growth rate of 4 cm/h and at compositions removed from the eutectic, i.e. 69.3 mol %  $Al_2O_3$ /30.7 mol %  $Y_3Al_5O_{12}$  which was rich in  $Y_3Al_5O_{12}$ , and 85.7 mol %  $Al_2O_3$ /14.3 mol %  $Y_3Al_5O_{12}$



Figure 2 Microstructure of 69.3 mol %  $Al_2O_3$ /30.7 mol %  $Y_3Al_5O_{12}$  composition solidified after heating to 1900° C. Temperature gradient = 190° C/cm, growth rate = 4 cm/h. Original magnification 500 ×.

which was rich in  $Al_2O_3$ , the microstructure consisted of primary phase and a fine eutectic dispersion. The microstructures of these compositions are shown in figs. 2 and 3 respectively. The primary phase in fig. 2 is  $Y_3Al_5O_{12}$ , and the primary phase in fig. 3 is  $Al_2O_3$ . This was verified



Figure 3 Microstructure of 85.7 mol %  $Al_2O_3$ /14.3 mol %  $Y_3Al_5O_{12}$  composition solidified after heating to 1950° C. Temperature gradient = 190° C/cm, growth rate = 4 cm/h. Original magnification 500 ×.

by scanning these polished sections for  $Y_{K\alpha}$  X-radiation with an electron probe microanalyser. Both primary phases appear to have grown in a faceted manner. Growth of the eutectic dispersion may be seen occurring from the primary  $Y_3Al_5O_{12}$  in fig. 2 whereas a ring of  $Y_3Al_5O_{12}$  surrounds the primary  $Al_2O_3$  in fig. 3. Sundquist and Mondolfo [15] have shown for metal systems that nucleation of eutectic on a primary phase indicates that this phase will nucleate first and cause nucleation of the second phase when coupled eutectic growth occurs. These photomicrographs indicate that  $Y_3Al_5O_{12}$  was the first phase to nucleate at the eutectic in the system  $Al_2O_3/Y_3Al_5O_{12}$ .

At growth rates between 2 and 13 cm/h and for the eutectic composition, 80.1 mol %  $Al_2O_3$  to 19.9 mol %  $Y_3Al_5O_{12}$ , the microstructure most commonly observed was the colony type. Figs. 4 and 5 are the longitudinal and transverse sections of an ingot of the eutectic composition grown at a rate of 4 cm/h. This microstructure arises because the liquid/solid interface is not planar as a result of the rejection of impurities ahead of the interface [16]. The most likely impurity would have been tungsten from the crucible. It was observed in this investigation that

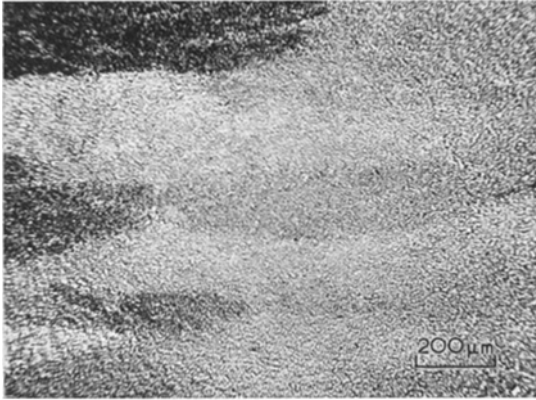


Figure 4 Longitudinal section of colony type microstructure of eutectic composition, 80.1 mol %  $\text{Al}_2\text{O}_3$ /19.9 mol %  $\text{Y}_3\text{Al}_5\text{O}_{12}$ , after heating to 1850 °C. Temperature gradient = 190 °C/cm, growth rate = 4 cm/h. Original magnification 125 ×.

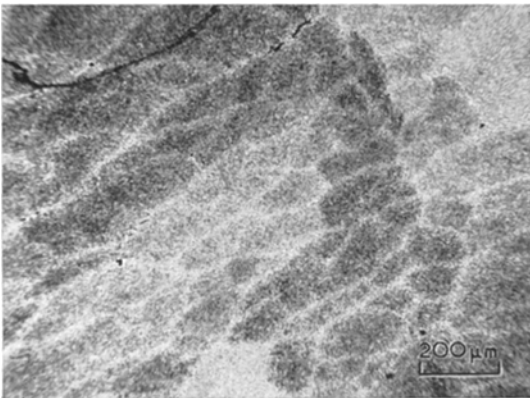


Figure 5 Transverse of colony type microstructure of eutectic composition, 80.1 mol %  $\text{Al}_2\text{O}_3$ /19.9 mol %  $\text{Y}_3\text{Al}_5\text{O}_{12}$ , after heating to 1850 °C. Temperature gradient = 190 °C/cm, growth rate = 4 cm/h. Original magnification 125 ×.

the melt did not attack the tungsten crucibles. It has been reported that the amount of tungsten found in sapphire single crystals pulled from a melt contained in a tungsten crucible was between 0.001 and 0.01 % [17]. X-ray fluorescence studies of an ingot of eutectic composition revealed that there was less than 0.1 % tungsten in these specimens. The solubility of tungsten metal or oxide in  $\text{Al}_2\text{O}_3$  and  $\text{Y}_3\text{Al}_5\text{O}_{12}$  is not known. The influence of the tungsten impurity on the shape of the liquid/solid interface could not be determined.

For ingots of the eutectic composition grown at rates greater than 4 cm/h, some of the colum-

nar grains exhibited highly oriented eutectic regions consisting of rods and platelets. Figs. 6 and 7 are longitudinal and transverse sections of such a grain. The spacing between rods is 2 μm.

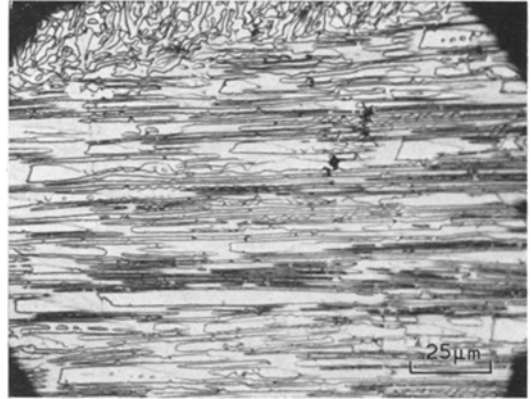


Figure 6 Longitudinal section of highly oriented eutectic microstructure of 80.1 mol %  $\text{Al}_2\text{O}_3$ /19.9 mol %  $\text{Y}_3\text{Al}_5\text{O}_{12}$  composition after heating to 1850 °C. Temperature gradient = 190 °C/cm, growth rate = 4 cm/h. Original magnification 1000 ×.

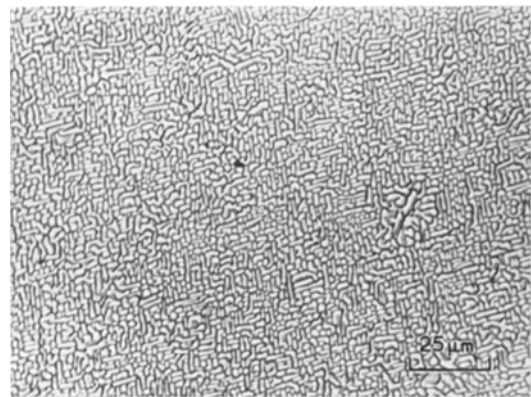


Figure 7 Transverse section of highly oriented eutectic microstructure of 80.1 mol %  $\text{Al}_2\text{O}_3$ /19.9 mol %  $\text{Y}_3\text{Al}_5\text{O}_{12}$  composition after heating to 1850 °C. Temperature gradient = 190 °C/cm, growth rate = 4 cm/h. Original magnification 1000 ×.

The rods and platelets are  $\text{Y}_3\text{Al}_5\text{O}_{12}$  in an  $\text{Al}_2\text{O}_3$  matrix. By comparing the electron probe microanalyser studies mentioned earlier with the optical studies, it was found that the  $\text{Y}_3\text{Al}_5\text{O}_{12}$  always appeared whiter when viewed under reflected light than the  $\text{Al}_2\text{O}_3$ . It was then easy to identify each phase in a photomicrograph. The existence of these highly oriented regions suggested that a

planar liquid/solid interface was at least present locally and that coupled growth can occur in this system. The columnar grain-structure of the ingot shows however that the liquid/solid interface was generally not planar. Also, the existence of both rods and platelets as shown in fig. 7 indicates that even when a planar liquid/solid interface was obtained locally, it tended to break down because of the impurities present [16].

Coupled eutectic growth does occur in the system  $\text{Al}_2\text{O}_3/\text{Y}_3\text{Al}_5\text{O}_{12}$  with a temperature gradient of  $190^\circ\text{C}/\text{cm}$  at growth rates above  $4\text{ cm/h}$ . The criteria of Hunt and Jackson [2] which limited coupled eutectic growth to low entropy of melting materials may not be suitable for oxides. The occurrence of faceted growth from the melt of the component phases may also be an insufficient criterion for prediction of a eutectic microstructure for the occurrence of facets is determined by the liquid/solid interface. While  $\text{Y}_3\text{Al}_5\text{O}_{12}$  normally grows in a faceted manner, Cockayne *et al* [18] have grown facet-free  $\text{Y}_3\text{Al}_5\text{O}_{12}$  by the Czochralski method by insuring that the liquid/solid interface was planar. Therefore the nature of the liquid/solid interface alone probably determines whether coupled eutectic growth occurs in a system, and that under conditions of a high temperature gradient coupled eutectic growth can occur in many non-metallic as well as metallic systems.

### Acknowledgements

The authors thank F. Cotter, W. Duffy, and A. Zani of the Army Materials and Mechanics Research Center for their help with the metallograph studies.

### References

1. G. A. CHADWICK, Proc. Joint Conf. on Solidification, Brighton, UK (December, 1967) to be published by British Institute of Metals.
2. J. D. HUNT and K. A. JACKSON, *Trans. Met. Soc. AIME* **236** (1966) 843.
3. C. B. ALCOCK and M. PELEG, *Trans. Brit. Ceram. Soc.* **66** (1967) 217.
4. H. YANAGIDA and F. A. KROGER, *Bull. Amer. Ceram. Soc.* **47** (1968) 366.
5. (a) O. N. CARLSON, W. D. MCMULLEN and E. D. GIBSON, US At. Energy Comm. IS-351 (1961) 26.  
(b) O. N. CARLSON and W. D. MCMULLEN, *ibid* IS-193 (1960) 40.
6. Janef Thermochemical Tables, The Dow Chemical Co., Midland, Mich, USA (March, 1964).
7. F. R. CHARVAT, J. C. SMITH and O. H. NESTOR, Proc. International Conf. on Crystal Growth, Boston (June, 1966) edited by H. Steffen (Pergamon, London, 1967) p. 45.
8. J. BASTERFIELD, M. J. PRESCOTT and B. COCKAYNE, *J. Materials Sci.* **3** (1968) 33.
9. D. VIECHNICKI and F. SCHMID, submitted to *Mat. Res. Bull.* (1968).
10. I. WARSHAW and R. ROY, *J. Amer. Ceram. Soc.* **42** (1959) 434.
11. L. E. OLDS and H. E. OTTO, private communication (December 1961) in "Phase Diagrams for Ceramists" by E. M. Levin, C. R. Robbins, and H. F. McMurdie (American Ceramic Society, Columbus, Ohio, 1964) p. 122.
12. N. A. TOROPOV, I. A. BONDAR, F. YA. GALKHOV, KH. S. NIKOGOSYAN and N. V. VINOGRADOVA, *Izv. Akad. Nauk. SSSR, Ser. Khim.* **7** (1964) 1158.
13. T. NOGUCHI and M. MIZUNO, *Kogyo Kagaku Zasshi* **70** (1967) 834.
14. A. D. KIRSHENBAUM and J. A. CAHIL, *J. Inorg. Nucl. Chem.* **14** (1960) 283.
15. B. E. SUNDQUIST and L. F. MONDOLFO, *Trans. Met. Soc. AIME* **221** (1961) 157.
16. B. CHALMERS, "Principles of Solidification" (Wiley New York, 1964) p. 207.
17. A. E. PALADINO and B. D. ROITER, *J. Amer. Ceram. Soc.* **47** (1964) 465.
18. B. COCKAYNE, M. CHESSWAS and D. B. GASSON, *J. Materials Sci.* **3** (1968) 224.